

Mechanism of Aluminum Sorption on Birnessite: Influences on Chromium (III) Oxidation

Scott E. Fendorf¹, Donald L. Sparks², and Mark Fendorf³. ¹Soil Science Division, University of Idaho, Moscow ID 83844, ²Department of Plant and Soil Sciences, University of Delaware, Newark DE 19717-1303, ³Department of Chemistry, University of California, Berkeley, CA 94720 USA.

Abstract

The oxidation of Cr(III) to Cr(VI) represents a significant environmental hazard due to the much greater mobility and toxicity of Cr(VI). Despite the importance of Cr(III) oxidation, many factors influencing this chemical process in soils and waters remain unknown. In this study we investigate the sorption mechanisms of Al on birnessite and their effects on Cr(III) oxidation. Aluminum had no effect on Cr(III) oxidation at pH values less than 4. However, at pH values greater than 4 Al effectively limited Cr(III) oxidation. Reacting Al with birnessite prior to the introduction of Cr(III) resulted in less oxidation than when both Al and Cr(III) were reacted simultaneously with birnessite. Prior reaction of birnessite with Al at pH 5, and 2.84 μmol s Cr(III) initially present, decreased oxidation from 2.80 to 0.28 μmol s Cr(VI). High-resolution transmission electron microscopy revealed that an aluminum hydroxide surface precipitate formed on birnessite at pH ≥ 4 , thus accounting for the observed sorption and electrophoretic mobility trends and Cr(III) oxidation inhibition. The amorphous $\text{Al}(\text{OH})_3$ surface precipitate formed at an ion activity product 10^3 times lower than for precipitation in bulk solution. Subsequent to the Al-MnO₂ reaction, introduction of Cr(III) resulted in a semicrystalline chromium hydroxide phase on the Al reacted birnessite. The resulting colloid was composed of three distinct metal-(hydr)oxides: $\delta\text{-MnO}_2$, $\text{Al}(\text{OH})_3 \cdot n\text{H}_2\text{O}$, and $\text{Cr}(\text{OH})_3 \cdot n\text{H}_2\text{O}$.

Introduction

Oxidation-reduction reactions dramatically affect the hazard of many compounds in the environment. Oxide/solution interfaces often influence redox reactions by allowing accelerated redox pathways, e.g., the oxygenation of metal ions (Davies and Morgan, 1989; Wehrli and Stumm, 1989) or by acting as an oxidant or reductant of a species present in soils and waters, e.g., the oxidation of small organic molecules (McBride, 1987; Stone, 1991). The oxidation of Cr(III) on manganese oxide surfaces has important implications for environmental quality since a rather benign species is transformed into a hazardous one.

Chromium is a redox reactive metal ion utilized in a variety of industrial processes; it has two stable oxidation states in the surface environment, Cr(III) and Cr(VI). Due to the lower toxicity and mobility of Cr(III) than Cr(VI), redox reactions affect the hazard and risk of Cr in soils. Chromium(VI) readily penetrates plant and animal cell membranes, is toxic as an oxidizing agent, and is a suspected carcinogen; consequently, the drinking water standard maximum for Cr is $10^{-6} M$ (U.S. EPA, 1984). Concentrations as low as 5 ppm Cr(VI) in soils and 0.5 ppm in solution can be toxic to plants (Turner and Rust, 1971). Furthermore, the anionic forms of Cr(VI) result in a greater mobility of this species than Cr(III) due to the low hydroxide solubility of Cr(III) and the abundance of negatively charged surfaces in soils. In contrast to Cr(VI), Cr(III) is not known to be toxic to plants and is essential in human nutrition (Bartlett and James, 1988). However, while Cr(III) was once considered relatively harmless in the environment, the potential for Cr(III) oxidation makes its hazard tantamount to that of Cr(VI).

Manganese oxides are one of the most reactive inorganic species present in surface environments, having pronounced effects on the redox status of soils or sediments (Bartlett, 1986). These oxides are the only known naturally occurring oxidant of Cr(III) at pH < 9 (Eary and Rai, 1987), and readily oxidize this species (Bartlett and James, 1979; Amacher and Baker, 1982; Eary and Rai, 1987; Fendorf and Zasoski, 1992). While recent investigations have thoroughly assessed Cr(III) oxidation by Mn-oxides in simple systems (Eary and Rai, 1987; Johnson and Xyla, 1991; Fendorf et al., 1992; Manceau and Charlet, 1992), influences of complex, multicomponent matrices of soils and waters have not been investigated. A knowledge of reaction conditions which affect Cr(III) oxidation is imperative for predicting the fate of Cr in soil and water systems, allowing one to determine conditions that facilitate or retard the formation of Cr(VI).

While the oxidation of Cr(III) by birnessite at pH < 4 continues until a reactant is limiting, the reaction is inhibited at higher pH values. Separate surface analysis studies (Fendorf et al., 1992b; Manceau and Charlet, 1992) confirmed that the source of Cr(III) oxidation inhibition was the formation of a $\text{Cr}(\text{OH})_3 \cdot n\text{H}_2\text{O}$ surface precipitate. The $\text{Cr}(\text{OH})_3$ surface precipitate inhibits Cr(III) oxidation by acting as a redox stable sink for Cr(III) and as a physical barrier between solution Cr(III) species and the oxidative Mn surface. Bidentate inner-sphere complexation of Cr(III) on Mn-oxides is the initial step in the redox reaction (Fendorf et al., 1992b). Hence, if a competing sorbate can inhibit Cr(III) complexation on manganese oxides the oxidation process may be hindered.

In the complex matrices of soils and waters, various species may be present that influence Cr(III) retention and, thus, oxidation by manganese oxides. Moreover, metal ions (Me), particularly Al, may form a solid solution with Cr(III)--as observed for Cr(III) and Fe(III) (Sass and Rai, 1987). The formation of a $\text{Cr,Me}(\text{OH})_3$ precipitate would limit the aqueous Cr(III) concentration and, if surface associated, would form a physical barrier between redox reactive Cr(III) and Mn(IV)/(III) species. This limitation in oxidation may be important in determining the potential for Cr(VI) production from Cr(III), which would thus decrease the potential hazard of Cr. Aluminum is common in many soil and water systems and its behavior in the surface environment is similar to that of Cr(III) (Bartlett and James, 1979, 1988). Accordingly, its effects on Cr(III) oxidation may have significant environmental implications. Furthermore, another trivalent ion, Fe(III), was observed to completely inhibit Cr(III) oxidation by $\delta\text{-MnO}_2$ (Amacher and Baker, 1982). Because of the potential formation of a solid solution and competitive sorption between Cr(III) and Al, the influences of Al on Cr(III) oxidation were investigated in this study. The objectives of this research were to determine: (i) the sorption mechanism and surface structure of Al on birnessite, (ii) the effects of Al on Cr(III) oxidation, and (iii) sorption mechanisms necessary to limit Cr(III) oxidation. Determining inhibitory factors in Cr(III) oxidation will enable a more comprehensive assessment of Cr hazards under specified conditions and may allow for the development of a safe disposal technique for this element.

Materials and Methods

The mineral birnessite ($\delta\text{-MnO}_2$) was prepared by the method of Buser et al. (1954). The specific surface area and zero point of charge (ZPC) were $223 \times 10^3 \text{ m}^2 \text{ kg}^{-1}$ and 2.7, respectively. X-ray diffraction studies of the birnessite, using a random powder mount, produced four broad peaks at 0.73, 0.36, 0.24, and 0.14 nm. These values are characteristic of $\delta\text{-MnO}_2$ and are in good agreement with those observed by others (Loganathan and Burau, 1973; Loganathan et al., 1977; Zasoski and Burau, 1988). Electron diffraction patterns confirmed the d-spacings obtained from X-ray diffraction, and high-resolution transmission electron microscope (HRTEM) images are representative of a synthetic birnessite. All chemicals that were used were reagent

grade, and metal solutions were made from their nitrate salts. The MnO_2 was suspended in 0.1M NaNO_3 at the desired pH value, which was maintained by addition of NaOH or HNO_3 .

Chromium(VI) was analyzed by the *s*-diphenyl carbazide method (Bartlett and James, 1979). Aluminum and Mn were analyzed using a sequential ICP-optical emission spectrophotometer.

Batch Studies

Batch methods were used to obtain steady state data. Supporting electrolytes were 0.1 M NaNO_3 . Twenty five mL of solution and 2.5 mg MnO_2 were placed in 50 mL polyethylene tubes to yield an initial solid concentration of 0.1 g L^{-1} . In noncompetitive sorption studies, the oxide was dispensed to the reaction vessel with the supporting electrolyte and allowed to hydrate for 24 h. After pH adjustment the metal ion of interest was added, with initial metal concentrations of 303 μM , and the total volume brought to 25 mL. The system was then mixed on a reciprocating shaker for 24 h after which an aliquot was withdrawn and the electrophoretic mobility (EM) of the particle measured with a Ranks Brothers apparatus. The remaining suspension was filtered through a 0.45 μm pore membrane filter, and the effluent was analyzed.

In competitive studies, the competing metal ion was added at an initial concentration of 290 μM to the oxide and supporting electrolyte after hydration. The system was allowed to react for 4 h prior to the addition of Cr(III); Cr(III) was then added and the sample was shaken for 24 h, filtered, and the effluent analyzed. All investigations were carried out over the pH range of 3 to 5 at 25 ± 3 °C. An N_2 (g) environment was maintained by initially bubbling N_2 (g) through the suspension and then keeping samples under an N_2 (g) stream. A portion of the final solid material in both competitive and non-competitive studies was removed for TEM analysis.

Electron Microscopy

High-resolution transmission electron microscopy (HRTEM) was performed on the solid material from systems of Al- MnO_2 and Al-Cr- MnO_2 . In this study, micrographs of MnO_2 reacted with 400 μM Al at pH 4 are shown in addition to a series of micrographs of the Al-Cr- MnO_2 systems. After the batch reactions, electron microscopy was performed by dispensing approximately 0.25 mL of the suspension on a holey carbon film supported by a copper mesh grid. The oxide coated grids were then rinsed with deionized water and air dried. Following this procedure HRTEM was performed on the specimens at 300 KeV using a Hitachi H-9000NAR transmission electron microscope, or at 200 KeV using a JEOL JEM200CX.

Results

Sorption of Al on Birnessite

The sorption of Al on birnessite, normalized to the surface area, is shown in Fig. 1 with solution pH ranging from 3 to 5. Aluminum sorption on birnessite occurred over the entire pH range (3 to 5), but a much more extensive increase in sorption occurs at pH > 4. The point where sorption increases dramatically (approximately pH 4) may represent a change in the sorption mechanism of Al.

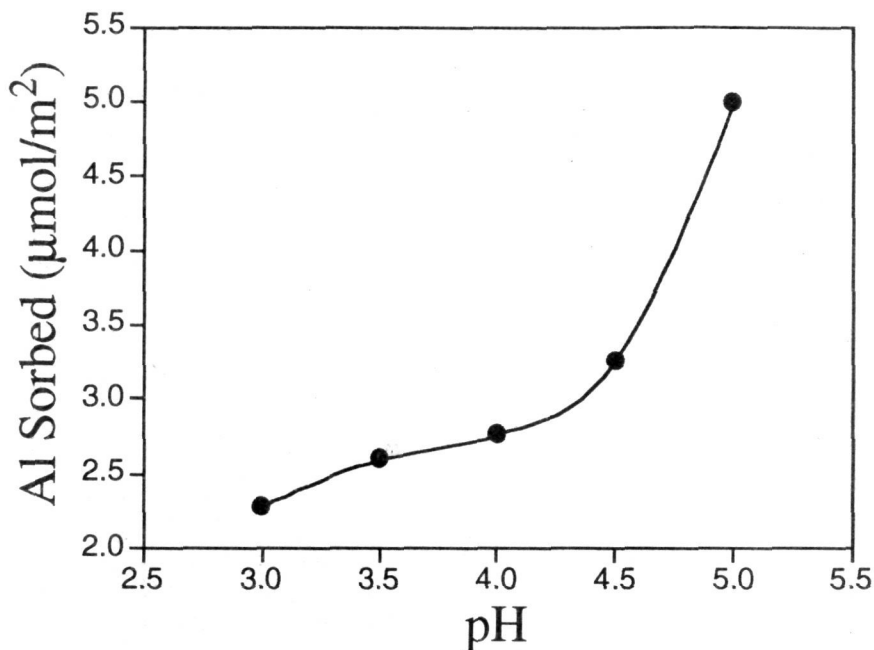


Figure 1. Aluminum retention on birnessite at initial concentrations of $303 \mu\text{M}$ in a matrix of 0.1 M NaNO_3 (Fendorf et al., 1993).

Aluminum induced a positive EM on birnessite throughout the pH range studied (Fig. 2). From pH 3 to 5, there are two relatively linear sections of the pH vs. EM data for the Al- MnO_2 system, similar to the EM of MnO_2 after reaction with Cr(III) (Fendorf and Zasoski, 1992). At pH 4, the positive slope of the EM vs. pH curve dramatically increased in the presence of Al. The point where the slope changes appears to represent the onset of a process which largely alters the surface properties of birnessite. This indicates a possible change in the sorption mechanism of Al. Electron micrographs of the MnO_2 surface prior to reaction and after reaction with $400 \mu\text{M}$ Al at pH 4 indicate a change in the surface structure of the oxide (Fig. 3).

The micrographs show that the unreacted material (Fig. 3a) was partially crystalline, with the characteristic balls of needles of synthetic birnessite depicted (McKenzie, 1977). Interspersed with amorphous material, an ordered needle-like morphology is characterized by layers of parallel atomic planes exhibiting severe bends and twists. In the images of the unreacted material, the needles are clearly delineated with no amorphous deposition. However, after reacting with Al at pH 4 a distinct change in the surface structure can be discerned. The needle-like morphology is still apparent, but the crystalline needles are no longer clearly delineated and an amorphous layer can be seen at the edges of the birnessite particles. Furthermore, a decrease in the clarity of the image is notable; this persisted over a range of focus settings bracketing the optimum value, indicating that the electron beam was incoherently scattered by an amorphous layer that coated the upper and/or lower surface(s) of the particle. Although a surface alteration is clearly discerned on birnessite at pH 4 ($400 \mu\text{M}$ Al), there are areas in the micrograph that remain clear and do not have amorphous material at their edges. Thus, amorphous $\text{Al}(\text{OH})_3$ formed discrete surface deposits (clusters) on birnessite at pH 4. Below pH 4 no surface modification was observed, and at pH 5

(400 μM Al) a more extensive surface deposition was observed in which the birnessite surface was entirely enveloped (Fendorf et al., 1992a). Therefore, HRTEM provides direct evidence that at an initial Al concentration of 400 μM , aluminum hydroxide surface precipitation occurs at pH 4. Surface precipitation is more extensive at pH 5 and completely envelops the manganese oxide.

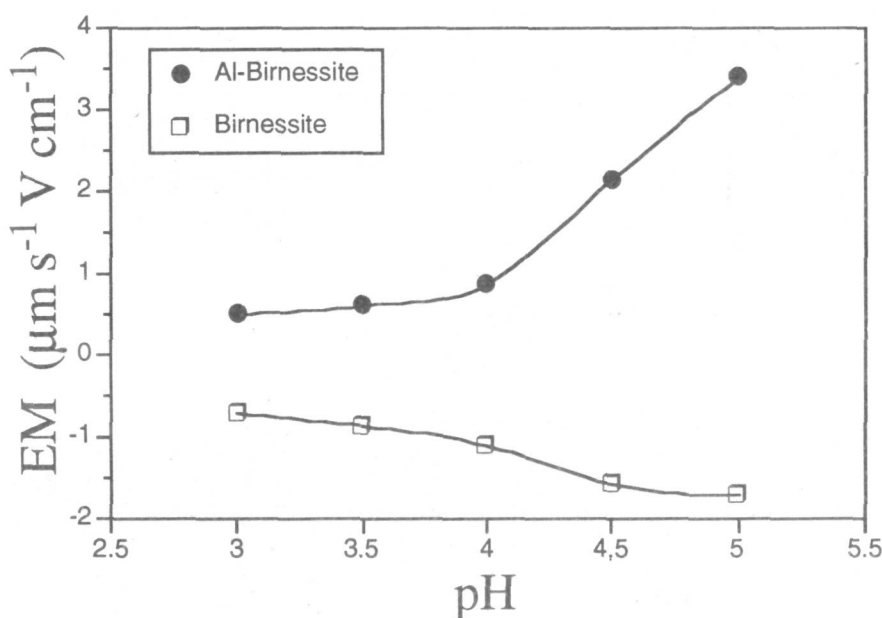


Figure 2. Electrophoretic mobility (EM) of birnessite after reaction with Al as a function of solution pH. The initial metal concentration was 303 μM (Fendorf et al., 1993).

Effects of Aluminum on Cr(III) Oxidation

The competitive sorption effects of 290 μM Al on the oxidation of Cr(III) were examined at pH 3 and 5 by reacting Al with birnessite prior to Cr(III) additions. The results are summarized in Table 1. At pH 3, Al did not affect Cr(III) oxidation. However, the effect of Al on Cr(III) oxidation at pH 5 was dramatic. With no Al present almost all the Cr(III) was oxidized at initial concentration of 73.3 μM (1.80 μmol s of the initial 1.84 μmol s Cr(III) were oxidized, 95%). In contrast, only 0.28 μmol s of the 18.4 μmol s Cr(III) (15%) were oxidized when birnessite was previously reacted with 290 μM Al. At higher initial Cr(III) concentrations, 615 μM (19.7 μmol s), prior reaction with 290 μM Al decreased the extent of oxidation from 2.76 μmol s (14%) to less than 0.74 μmol s (4%). The chemical equilibrium program MINTQA2 (Allison et al., 1990) predicted that 290 μM Al would be slightly over-saturated with respect to $\text{Al}(\text{OH})_3$ (am) at pH 5. However, although saturation was predicted solution precipitation was never observed in identical solutions without birnessite present.

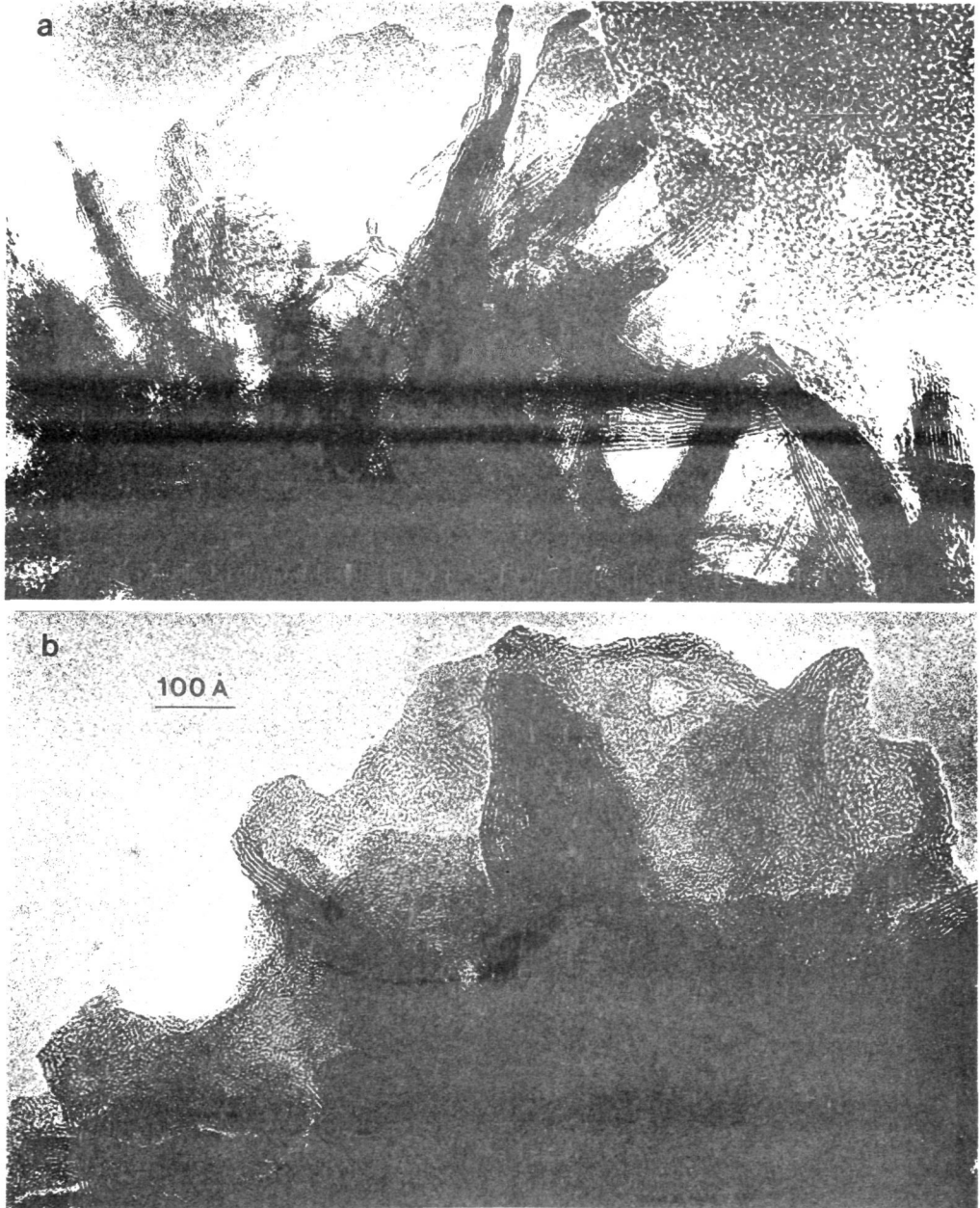


Figure 3. High-resolution electron micrograph of birnessite (a) prior to reaction and (b) after reaction with $400 \mu\text{M}$ Al at pH 4. After reaction (b), amorphous deposition of Al-hydroxide is observed along the edges of the particle.

Table 1. Competitive effects of Al on Cr(III) oxidation by birnessite at pH 3 and 5. The initial concentration of Al was 290 μM (data from Fendorf et al., 1993).

pH	Cr(III) ₀ ^a	Competing Ion	Cr(VI) ^b	%Oxidation
3	1.83	none	1.69 ± 0.08	92.3
		Al(III)	1.70 ± 0.12	93.1
	15.38	none	9.24 ± 0.50	60.1
		Al(III)	9.06 ± 0.65	58.9
5	1.83	none	1.74 ± 0.029	95.0
		Al(III)	0.273 ± 0.020	14.9
	15.38	none	2.15 ± 0.12	14.0
		Al(III)	0.61 ± 0.018	3.98

^a Initial Cr(III) level (μmoles)

^b μmoles

To further evaluate the effects of Al on Cr(III) oxidation by birnessite, a more extensive range of concentration and pH values was investigated. Figure 4 illustrates the effects of Al over the pH range of 3 to 5 with Al concentrations of 40, 200, and 400 μM . In Fig. 4, the extent of Cr(III) oxidation is shown by the amount of Cr(VI) produced as a function of the saturation index ($SI = \log IAP/K_{sp}$, where IAP is the ion activity product) for $\text{Al}(\text{OH})_3$ (am), calculated using MINTEQA2. Although the formation of crystalline $\text{Al}(\text{OH})_3$ phases (e.g., diaspore, boehmite, or gibbsite) would be thermodynamically more favorable, an amorphous surface precipitate was discerned with HRTEM. Small microcrystalline domains were discerned in the aluminum hydroxide precipitate, but it was dominantly an amorphous phase. This necessitated the employment of $SI_{\text{Al}(\text{OH})_3}$ (am). Kinetic rather than thermodynamic constraints often are the controlling factor in precipitation reactions and appear to govern the reaction under these conditions.

As the $SI_{\text{Al}(\text{OH})_3}$ (am) increased the extent of oxidation decreased, and as saturation with respect to $\text{Al}(\text{OH})_3$ (am) was approached oxidation became almost negligible (Fig. 4). The formation of an aluminum hydroxide surface precipitate coincided with Al induced Cr(III) oxidation inhibition (Fig. 3); complete aluminum hydroxide surface coverage at pH 5 (Fendorf et al., 1992) almost totally inhibits Cr(III) oxidation. Therefore, $\text{Al}(\text{OH})_3$ surface nucleation inhibits Cr(III) oxidation and may explain the sorption and EM of Al.

Surface Effects of Sorbed Al

Of the metal ions investigated only Al affected the extent of Cr(III) oxidation; the source of inhibition was the formation of an $\text{Al}(\text{OH})_3$ (am) surface precipitate on birnessite. To further explore the conditions under which this important oxidation inhibition mechanism occurs, and to determine surface modifications induced by this reaction, HRTEM analyses were performed on the reaction systems that are depicted in Fig. 4.

Competitive adsorption of Al with Cr(III) does not appear to influence the production of Cr(VI), as shown by the limited affect Al had on Cr(III) oxidation at lower pH values. Because Al surface precipitation appears to be the controlling factor influencing the oxidation reaction, the

production of Cr(VI) as a function of the SI for $\text{Al}(\text{OH})_3$ should be useful for ascertaining conditions which invoke surface precipitation. The extent of oxidation begins decreasing at a SI of -3 (Fig. 4), with a sharp sigmoidal decrease in Cr(VI) production continuing until negligible oxidation occurs at a SI of approximately -0.3. Therefore, it appears that metal-hydroxide nucleation occurs at an IAP 10^3 times lower (SI = -3.0) than is predicted for $\text{Al}(\text{OH})_3$ (am) in bulk solution.

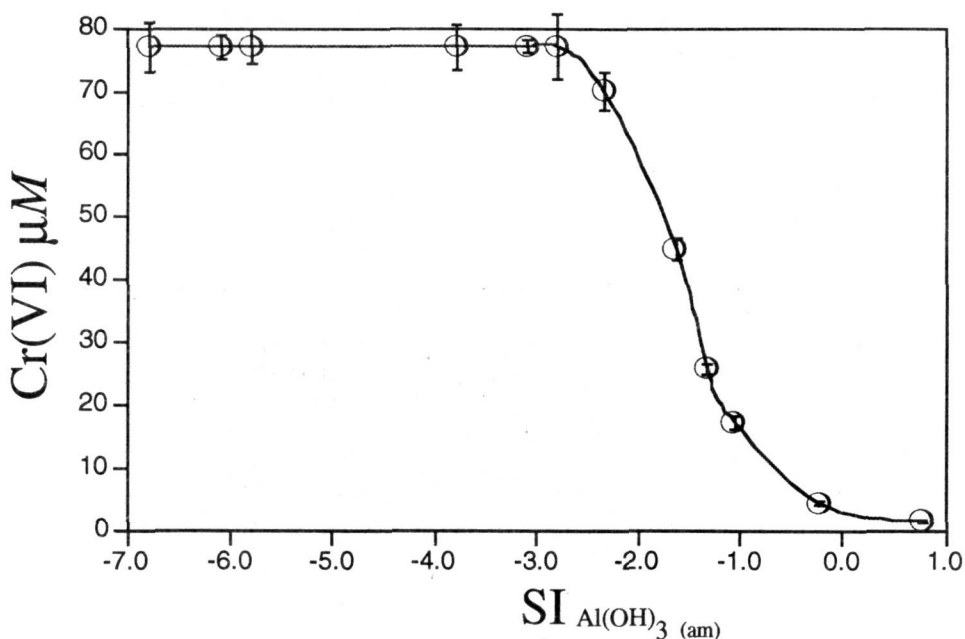


Figure 4. The effect of Al on Cr(III) oxidation by birnessite expressed by Cr(VI) production as a function of the saturation index (SI) for $\text{Al}(\text{OH})_3$ (am). Reactions were carried out at initial Al concentrations of 40, 200, and 400 μM at pH 3.0, 4.0, 4.5, and 5.0 with 77 μM Cr(III).

The dramatic decrease in Al solubility at the solid/solution interface may result from a coprecipitated $\text{Al,Cr}(\text{OH})_3$ phase rather than from a pure $\text{Al}(\text{OH})_3$ (am) phase. Sass and Rai (1987) found that $\text{Fe,Cr}(\text{OH})_3$ phases readily precipitate and decreased the solubility of Fe by the amount of Cr present, i.e., the hydroxide solubility of Fe(III) is then governed by an IAP which is a function of Fe(III), OH, and Cr(III) activities. However, in the systems which are described in Fig. 4, Al was reacted with birnessite prior to the addition of Cr(III). Thus, the potential for a Al-Cr solid solution would decrease. Nonetheless, one cannot rule out the possible formation of a coprecipitate, nor can one definitively confirm the presence of a surface precipitate using only a macroscopic analysis. Accordingly, to further examine the previously defined systems we employed electron microscopy to explore whether the precipitation of a surface $\text{Al}(\text{OH})_3$ (am) phase resulted at an SI of -3, and to determine if a coprecipitate of Al-Cr occurred.

At a SI of less than -3.1, HRTEM images indicated that no alteration of the birnessite surface occurred (Fig. 3a). However, as the SI increased above -3.0 a surface alteration can be discerned that progressively becomes more extensive at higher SI values (Fig. 5). In the systems reacted with Cr(III) and Al (Fig. 5), the deposition of an amorphous layer can be seen at the edges of the crystalline MnO₂ needles. At SI -2.32 (Fig. 5a), the deposited material is predominantly amorphous, although there are areas shown which do indicate slight ordering (semicrystalline). The amorphous deposits ranged from less than 1 to greater than 10 nm in thickness. The amorphous material is not uniformly distributed on birnessite. Some areas have extensive coverages (layer depths > 10 nm) and thus completely insulate the oxide surface from the solution. Other areas have little precipitate and would appear to possibly remain reactive with the solution. This would explain the degree of oxidation depicted in Fig. 4; oxidation was decreased but still occurred in appreciable amounts. The heavily deposited areas would not be redox reactive with Cr(III), in contrast to the high reactivity of the exposed portions of manganese oxide.

The HRTEM analysis showed that further increases in SI enhanced the deposition of the new solid phase. Figure 5b illustrates that under conditions which represent approximately the half height point (SI = -1.32) on the SI vs Cr(VI) sigmoidal curve (Fig. 4), extensive growths of the new material are observed at the edges of the MnO₂ particle. In addition, the decrease in image clarity was more pronounced, suggesting the presence of a thicker surface layer, but areas remain which have relatively little coatings. In contrast, at SI of 0.78 (Fig. 5c) a gross change in the particle occurred. The remnant birnessite is only partially imaged and there is a vast amount of the newly formed phase which completely encapsulates the original MnO₂ particle. The newly formed phase is extensive enough to largely inhibit the imaging of the crystalline MnO₂ needles and would mask its properties from the surrounding solution. Even low magnification images (Fig. 6) reveal an extensive surface precipitate.

The newly deposited material after reaction with Al and Cr(III) is predominantly amorphous; however, in all of the micrographs there are many areas which exhibit some atomic-ordering (crystallinity). Both the extent and degree of ordering is greater in the Cr(III)-Al reacted systems compared to the manganese oxide reacted only with Al (Fig. 3b). Isolating an area of the solid material depicted in Fig. 5c provides evidence for the observed microcrystallinity (Fig. 7). In Fig. 7 partial atomic ordering can be clearly seen in the outer 5 nm. A distinct phase boundary occurs between 10 and 20 nm from the surface with the interior phase being almost exclusively amorphous (crystalline MnO₂ needles are out of the plane of view but would reside just below the bottom of the depicted image). It would appear that other semicrystalline areas of these solids would be due to the deposition of chromium hydroxide on an aluminum hydroxide phase which had previously formed. The chromium hydroxide would thus also account for the areas of microcrystallinity depicted throughout Fig. 5.

Although small amounts of an Al,Cr-(OH)₃·nH₂O coprecipitate may have formed, single metal hydroxides appear to be the main materials present in these systems--with distinct phase boundaries separating them. That is not to say that an Al,Cr(OH)₃·nH₂O solid-solution is not possible (or even probable under the appropriate reaction conditions), but rather, the reaction of Al with birnessite prior to the introduction of Cr(III) promoted the formation of separate solid phases. Consequently, surface precipitation of Al(OH)₃ was possible without the influences of Cr(III). This was followed by the introduction of Cr(III) which formed a second surface precipitate on the aluminum hydroxide, as clearly demonstrated by the HRTEM analyses.

Discussion

The oxidation of Cr(III) by birnessite is limited at pH ≥ 4 when Cr(III) concentrations exceed 77 μM (Fendorf and Zasoski, 1992). The presence of Al also limited Cr(III) oxidation at pH values greater than 4; at lower pH values Al had no effect (Table 1). Thus, both Cr(III) and Al limit Cr(III) oxidation by manganese oxides at higher pH values. The inhibitory mechanism can be

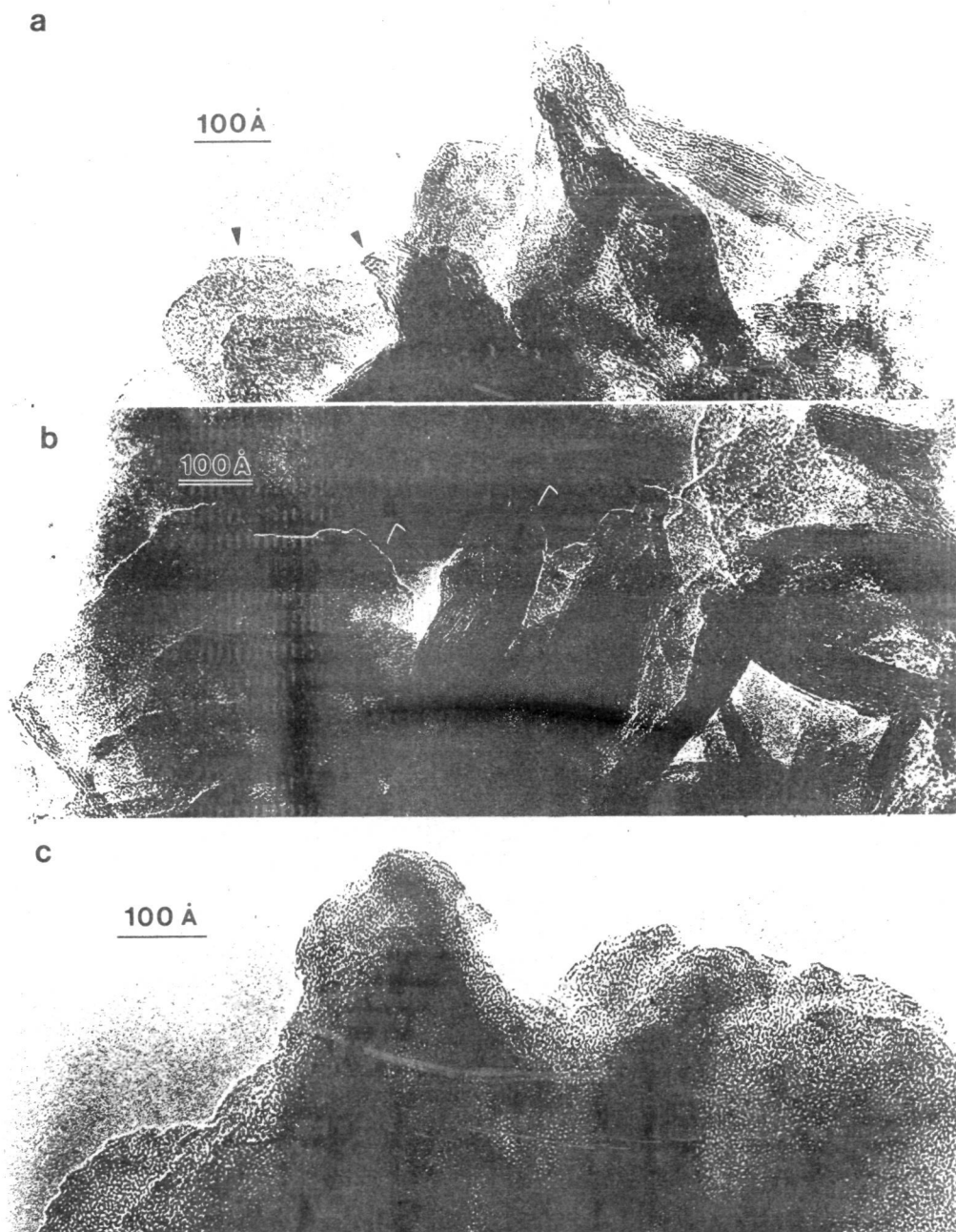


Figure 5. Solid-phase deposition on birnessite induced by reaction with $77 \mu\text{M}$ Cr(III) and (a) $40 \mu\text{M}$ Al, pH 4 (SI = -2.32), (b) $400 \mu\text{M}$ Al, pH 4.5 (SI = -1.32), and (c) $400 \mu\text{M}$ Al, pH 5 (SI = 0.78).

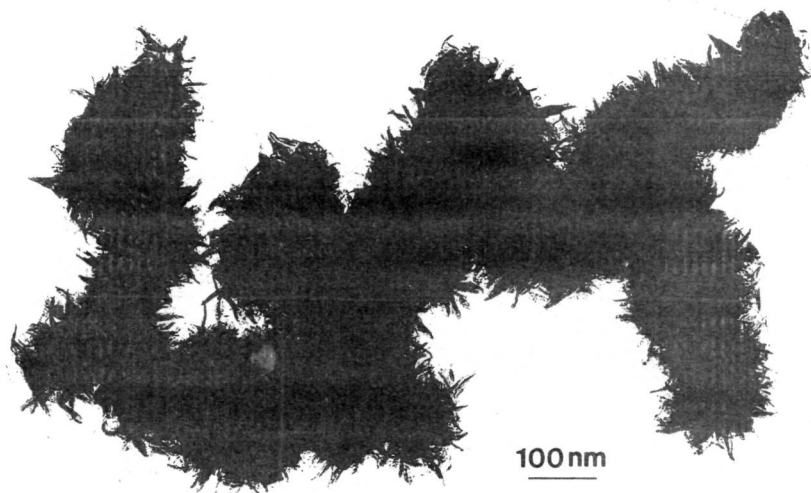


Figure 6. Low magnification HRTEM image of birnessite after reaction with 50 μM Al and 77 μM Cr(III) at pH 4.5.

attributed to surface precipitation based on the following observation. Aluminum invoked a strong charge reversal on birnessite at pH values greater than 4, as was observed with Cr(III) (Fendorf and Zamoski, 1992). Additionally, a dramatic change in the slope of the EM vs. pH curve occurred over the pH range of 3 to 5 in the presence of Al. And finally, HRTEM images revealed the presence of a surface precipitate on birnessite after reaction with Al and/or Cr(III).

At pH values exceeding 4 the hydrolysis products of either Al or Cr(III) may bind to the oxide surface in a manner which inhibits the redox reaction between MnO_2 and Cr(III). It is well established that the hydrolysis of metal ions affects their sorption (Schindler and Stumm, 1987). The results of this study, however, impart another criterion on the sorption mechanism of Al and Cr(III) at higher pH values: the resulting surface species inhibited the redox reaction of Cr(III)- MnO_2 . Inhibition of Cr(III) oxidation was correlated with conditions favoring the hydrolysis products of Al or Cr(III). Table 2 lists the proportions of monomeric hydrolysis species present in solution for the various metal ions used, as calculated by MINTEQA2. One must recognize that in the electrified solid/solution interface, solution hydrolysis constants may not be representative of interfacial hydrolysis reactions (James and Healy, 1972). Although precipitation was never observed in solution under the reaction conditions employed, aluminum or chromium hydroxide surface precipitation may be expected due to surficial influences; this results from the lowering of solvation energies by the electrified interface or surface complex).

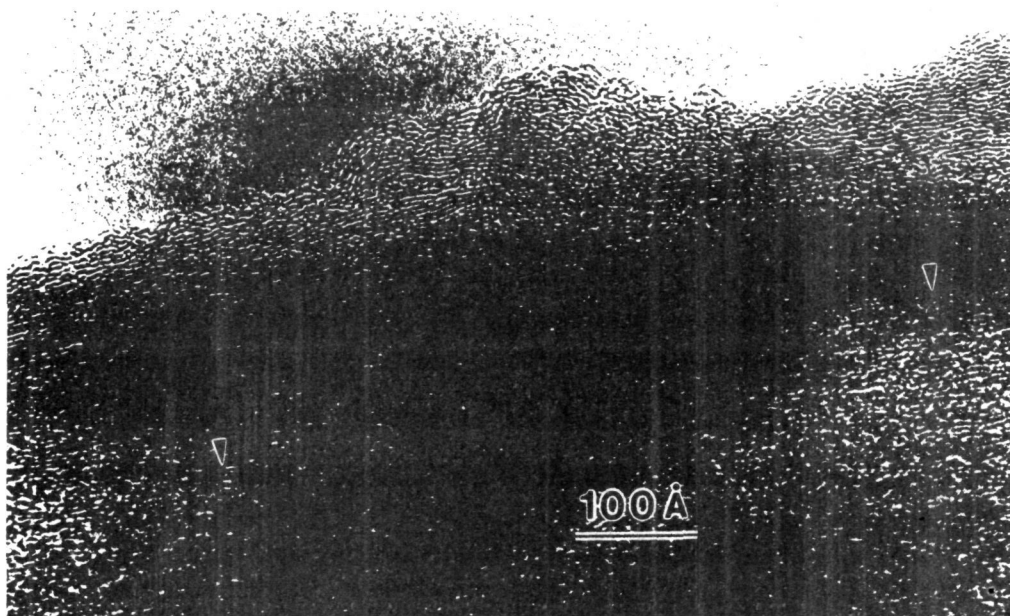


Figure 7. Phase boundary (marked by arrows) between the deposited $\text{Al}(\text{OH})_3$ (am) material and $\text{Cr}(\text{OH})_3 \cdot n\text{H}_2\text{O}$. The $\delta\text{-MnO}_2$ phase is out of the plane of view, but resides slightly below the imaged material.

The polymerization of Al species may occur at the higher Al concentrations and pH values investigated; however we did not attempt to quantitatively address polymerization as free energy of formation data are not known or reliable. In addition, published data indicates polynuclear Cr(III) species are insignificant under conditions employed in this study (Rai et al., 1987). Here, MINTEQA2 was used only to predict the proportions of monomeric hydrolysis species. The modeling was conducted to exemplify the correlation between the hydrolysis products and sorption and EM (Table 2).

Various researchers have shown that surface precipitation occurs prior to bulk precipitation (James and Healy, 1972; Tewari and Lee, 1975; Murray and Dillard, 1979; Crowther et al., 1982; Charlet and Manceau, 1992). James and Healy (1972) theorized that incorporating electric field effects of surfaces into the free energies of reaction greatly reduces the metal hydroxide's solubility in the interfacial region. Based on the surface charge of $\delta\text{-MnO}_2$, Murray and Dillard (1979) used the model developed by James and Healy (1972) and calculated that the solubility of metal hydroxides was reduced by at least 10^2 in the interfacial region. In our study, it also is apparent that while Cr(III) and Al did not precipitate in solution, surface catalyzed nucleation did occur. Therefore, the macroscopic data of Fig. 4 fully agree with the results of Murray and Dillard (1979) and indicate that solubility constants are lowered by as much as 10^3 in the interfacial region of birnessite.

Table 2. Speciation of solution components as a function of pH, calculated by the computer program MINTEQA2.

Component	pH	Percent Species
Al(III)	3	97.4 Al ³⁺
		2.6 Al(OH) ⁺²
	4	60.1 Al ³⁺
		39.9 Al(OH) ⁺²
	5	7.1 Al ³⁺
		64.2 Al(OH) ⁺²
	28.7 Al(OH) ₂ ⁺	
Cr(III)	3	92.3 Cr ⁺³
		7.7 Cr(OH) ⁺²
	4	53.9 Cr ⁺³
		45.1 Cr(OH) ⁺²
	5	8.9 Cr ⁺³
		74.8 Cr(OH) ⁺²
	16.1 Cr(OH) ₂ ⁺	

The change in slope of the Al-MnO₂ EM vs. pH curve may be due to a change in the sorption mechanism of Al on birnessite. Below pH 4, Al may bind at isolated sites, while near pH 4 multinuclear species may begin to form, followed by a progression to complete surface precipitation at higher pH values. Bleam and McBride (1986) noted a progression from isolated site binding of Mn(II) to the formation of Mn(OH)₂ surface clusters. They postulated that mass action balance governed the sorption mechanism. Furthermore, Farley et al. (1985) have thermodynamically modeled the progression from isolated site binding to the formation of surface precipitates. Recent extended X-ray absorption fine structure (EXAFS) spectroscopic studies indicate that Pb(II) and Co(II) form multinuclear species on oxide surfaces at about 10% surface coverage (Brown et al., 1989), and Cr(III) also forms multinuclear species on hydrous ferric oxide (Charlet and Manceau, 1992), δ-MnO₂ (Manceau and Charlet, 1992), and silica (Fendorf et al., 1994). At pH 5, a surface precipitate of aluminum hydroxide has been observed (Fendorf et al., 1992a) and surface clusters were observed in this study at pH 4. Therefore, it seems plausible that a progression from isolated site binding at low pH values (pH < 4) to multinuclear species (pH 4) and finally surface precipitation at higher pH values (pH > 4) occurs. The sorption mechanism seems to correlate with the SI for Al(OH)₃ (am) and would account for the observed EM trends and Al-induced effects on Cr(III) oxidation.

The formation of a surface nucleated metal-hydroxide phase would explain the inhibition in Cr(III) oxidation. At higher initial metal concentrations, surface quantities of Cr and Al were sufficient to approach and exceed a monolayer coverage based on their respective hydrated radii. The sharp increase in EM induced by Al (Fig. 2) and Cr(III) (Fendorf and Zasoski, 1992) at a critical pH value would represent the onset of Al- or Cr(OH)₃ surface precipitate. The precipitated Al- or Cr(OH)₃ would mask the properties of the birnessite and inhibit subsequent Cr(III)

oxidation. This would account for the changes in the EM and oxidation inhibition induced by Al on δ -MnO₂.

Our results (Fendorf et al., 1992b) and those of Manceau and Charlet (1992) indicate that Cr(OH)₃ • nH₂O formed on birnessite at pH ≥ 4 and solution Cr(III) concentrations exceeding 400 μM. Precipitation was not observed in solution and therefore must have been surface catalyzed. Inner-sphere surface complexation of the Cr(III) forming the surface precipitate would be restricted, as oxidation of Cr(III) would occur prior to nucleation. Thus, Cr(OH)₃ nucleation must have occurred in the interfacial region but at a distance great enough to prohibit electron transfer between surface Mn(IV)/Mn(III) and interfacial Cr(III). This indicates that electrostatic effects catalyzed the precipitation reactions. Surface precipitation reactions involving Al may be similar to Cr(III) because of similar hydrolysis constants and hydroxide solubility. This postulate is supported by the HRTEM results which show that a surface precipitate of Al(OH)₃ also occurred on birnessite.

Conclusions

Aluminum decreased the extent of Cr(III) oxidation by birnessite but only at pH values greater than 4. Under these reaction conditions HRTEM analysis revealed that a surface precipitate of an amorphous aluminum hydroxide formed on the birnessite surface. The results of the HRTEM analysis confirm the hypothesis based on the macroscopic trends of the saturation index plot. In fact, surface precipitation of Al(OH)₃ (am) occurs at an IAP 10³ times lower than would be expected for this reaction in solution. With increased Al concentrations surface precipitation was enhanced; at pH 5 with 400 μM Al present a surface precipitate formed that completely enveloped the manganese oxide.

When Cr(III) was reacted with the Al(OH)₃-MnO₂ particle its oxidation was inhibited and a second surface precipitate resulted: a Cr(OH)₃•nH₂O. This precipitate was semicrystalline and deposited on the aluminum hydroxide surface precipitate. Thus, the resulting conglomerated colloid is composed of three distinct metal-(hydr)oxide phases: MnO₂, Al(OH)₃ (am), and Cr(OH)₃ • nH₂O, with possibly slight amounts of an Al,Cr(OH)₃ coprecipitate. At the lower SI where precipitation occurred, the solution would experience physical/chemical attributes of all three phases, while at higher SI, properties exerted by the chromium and aluminum hydroxides would influence interfacial processes. Surface precipitation would not be expected to occur at the lowest pH values that were studied. This explains the absence of an Al effect on Cr(III) oxidation at pH < 4. Consequently, it appears that surface nucleation is necessary to inhibit Cr(III) oxidation.

Acknowledgements

We would like to greatly acknowledge support for this project from the NRI Competitive Grants Program/USDA, award number 93-37102-9481.

References

- Allison, J.D., D.S. Brown, D.S., and K.J. Novo-Gradac. 1990. MINTEQA2/PRODEFA2, A Geochemical Assessment Model for Environmental Systems: Version 3.0. U.S. Environmental Protection Agency: Athens, Georgia.
- Amacher, M.C., and D.A. Baker. 1982. Redox reactions involving chromium, plutonium, and manganese in soils, Final report DE-ASO8-77DPO4515; Institute for Research on Land & Water Resources: Penn. State University.

- Bartlett, R.J. 1986. Soil redox behavior. pp. 179-207. *In* D.L. Sparks (ed.) Soil physical chemistry. CRC Press, Boca Raton, FL.
- Bartlett, R.J., and B.R. James. 1988. Mobility and bioavailability of chromium in soils. pp. 267-303. *In* J.O. Nriagu and E. Nieborer (eds.) Chromium in the natural and human environments. Wiley and Sons, New York.
- Bartlett R.J., and B. James. 1979. Behavior of chromium in soils: III. Oxidation. *J. Environ. Qual.* **8**: 31-35.
- Bleam, W.F., and M.B. McBride. 1986. The chemistry of adsorbed Cu(II) and Mn(II) in aqueous titanium dioxide suspensions. *J. Colloid Interface Sci.* **103**: 124-132.
- Brown, G.E., Jr., G.A. Parks, and C.J. Chisholm-Brause. 1989. In-situ x-ray absorption spectroscopic studies of ions at oxide-water interfaces. *Chimia.* **43**: 248-256.
- Buser, W., P. Graf, and W. Feitknecht. 1954. Beitrag zur kenntis der mangan (II)- manganit und des δ -MnO₂. *Helv. Chim. Acta.* **37**: 2322-2333.
- Charlet, L. and A.A. Manceau. 1992. X-ray absorption spectroscopic study of the sorption of Cr(III) at the oxide-water interface: I. Molecular mechanism of Cr(III) oxidation on Mn oxides. *J. Colloid Interface Sci.* **148**: 425-442.
- Crowther, D.L., J.G. Dillard, and J.W. Murray. 1983. The mechanism of Co(II) oxidation on synthetic birnessite. *Geochim. Cosmochim. Acta.* **47**: 1399-1403.
- Davies, S.H.R., and J.J. Morgan. 1989. Manganese(II) oxidation kinetics on oxide surfaces. *J. Colloid Interface Sci.* **129**: 63-77.
- Eary, L.E., and D. Rai. 1987. Kinetics of chromium(III) oxidation to chromium(VI) by reaction with manganese dioxide. *Environ. Sci. Technol.* **21**:1187-1193.
- Farley, K.J., D.A. Dzombak, and F.M.M. Morel. 1985. A surface precipitation model for the sorption of cations on metal oxides. *J. Colloid Interface Sci.* **106**:226-242.
- Fendorf, S.E., and R.J. Zasoski. 1992. Chromium(III) oxidation by δ -MnO₂: I. Characterization. *Environ. Sci. Technol.* **26**:79-85.
- Fendorf, S.E., M. Fendorf, R. Gronsky, and D.L. Sparks. 1992a. Surface precipitation reactions on oxide surfaces. *J. Colloid Interface Sci.* **148**: 295-298.
- Fendorf, S.E., M. Fendorf, D.L. Sparks, and R. Gronsky. 1992b. Inhibitory mechanism of Cr(III) oxidation. *J. Colloid Interface Sci.* **148**: 37-54.
- Fendorf, S.E., R.J. Zasoski, and R.G. Burau. 1993. Competitive metal effects on Cr(III) oxidation by birnessite. *Soil Sci. Soc. Am. J.* **58**: In Press
- Fendorf, S.E., G.M. Lamble, M.G. Stapleton, M.J. Kelley, and D.L. Sparks. 1994. Mechanisms of chromium(III) sorption on silica. I: Cr(III) surface structure derived by extended x-ray absorption fine structure spectroscopy. *Environ. Sci. Technol.* In Press.
- James, R.O., and T.W. Healy. 1972. Adsorption of hydrolyzable metal ions at the oxide-water interface: II. Charge reversal of SiO₂ and TiO₂ colloids by adsorbed Co(II), La, and Th(IV) as model systems. *J. Colloid Interface Sci.* **40**:53-64.

- Johnson, C.A., and A.G. Xyla 1991. The oxidation of chromium(III) to chromium(VI) on the surface of manganate (γ -MnOOH). *Geochim Cosmochim Acta*. **55**:2861-2866.
- Loganathan, P., and R.G. Burau. 1973. Sorption of heavy metal ions by a hydrous manganese oxide. *Geochim. Cosmochim. Acta*. **37**:1277-1294.
- Loganathan, P., R.G. Burau, and D.W. Furstenu. 1977. Influences of pH on the sorption of Co^{2+} , Zn^{2+} and Ca^{2+} by a hydrous manganese oxide. *Soil Sci. Soc. Am. J.* **41**: 57-62.
- Manceau, A.A., and L. Charlet. 1992. X-ray absorption spectroscopic study of the sorption of Cr(III) at the oxide-water interface: II. Adsorption, coprecipitation, and surface precipitation on hydrous ferric oxide. *J. Colloid Interface Sci.* **148**: 443-458.
- McBride, M.B. 1987. Adsorption and oxidation of phenolic compounds by iron and manganese oxides. *Soil Sci. Soc. Am. J.* **51**: 1466-1472.
- McKenzie, 1977. Manganese oxides and hydroxides. pp. 181-193. In J.B. Dixon (ed.) Minerals in the soil environment. Soil Sci. Soc. Am, Madison WI.
- Murray, J.W., and J.G. Dillard. 1979. The oxidation of cobalt(II) adsorbed on manganese dioxide. *Geochim. Cosmochim. Acta*. **43**:781-787.
- Rai, D., B.M. Sass, and D.A. Moore. 1987. Chromium(III) hydrolysis constants and solubility of chromium(III) hydroxide. *Inorg. Chem.* **26**:345-349.
- Sass, B.M., and D. Rai. 1987. Solubility of amorphous chromium(III)-iron(III) hydroxide solid solutions. *Inorg. Chem.* **26**:2228-2232.
- Stone, A.T. 1991. Oxidation and hydrolysis of ionizable organic pollutants at hydrous metal oxide surfaces. pp. 231-254. In D.L. Sparks and D.L. Suarez (eds.) Rates of soil chemical processes. Soil Sci. Soc. Am. Special Publication, Madison, WI.
- Schindler, P.W., and W. Stumm. 1987. The surface chemistry of oxides, hydroxides, and oxide minerals. pp. 83-110. In W. Stumm (ed.) Aquatic surface chemistry. Wiley and Sons, New York.
- Tewari, P.H., and W.J. Lee. 1975. Adsorption of Co(II) at the oxide-water interface. *J. Colloid Interface Sci.* **52**:77-88.
- Turner, M.A., and R.H. Rust. 1971. Effects of chromium on growth and mineral nutrition of soybeans. *Soil Sci. Soc. Am. Proc.* **35**:755-758.
- U.S. EPA. 1984. Code of federal regulations Title 40, national interim primary drinking water regulations, Part 141. U.S. EPA, Washington, D.C.
- Wehrli, B., and W. Stumm. 1989. Vanadyl in natural waters: adsorption and hydrolysis promoted oxygenation. *Geochim. Cosmochim. Acta*. **53**: 69-77.
- Zasoski, R.J., and R.G. Burau. 1988. Sorption and sorptive interactions of cadmium and zinc on hydrous manganese dioxide. *Soil. Sci. Soc. Am. J.* **52**:81-87.